Submillimeter lung MRI at 0.55 T using balanced steady-state free precession with half-radial dual-echo readout (bSTAR)

Grzegorz Bauman[1,2] | **Nam G. Lee**[3] | **Ye Tian**[4] | **Oliver Bieri**[1,2] |
Krishna S. Nayak[3,4]

[1]Division of Radiological Physics, Department of Radiology, University of Basel Hospital, Basel, Switzerland

[2]Department of Biomedical Engineering, University of Basel, Basel, Switzerland

[3]Department of Biomedical Engineering, Viterbi School of Engineering, University of Southern California, Los Angeles, California, USA

[4] Ming Hsieh Department of Electrical and Computer Engineering, Viterbi School of Engineering, University of Southern California, Los Angeles, California, USA

Correspondence
Grzegorz Bauman, Department of Radiology, University Hospital Basel, Petersgraben 4, Basel 4031, Switzerland.
Email: grzegorz.bauman@usb.ch

Purpose: To demonstrate the feasibility of high-resolution morphologic lung MRI at 0.55 T using a free-breathing balanced steady-state free precession half-radial dual-echo imaging technique (bSTAR).

Methods: Self-gated free-breathing bSTAR ($TE_1/TE_2/TR$ of 0.13/1.93/2.14 ms) lung imaging in five healthy volunteers and a patient with granulomatous lung disease was performed using a 0.55 T MR-scanner. A wobbling Archimedean spiral pole (WASP) trajectory was used to ensure a homogenous coverage of k-space over multiple breathing cycles. WASP uses short-duration interleaves randomly tilted by a small polar angle and rotated by a golden angle about the polar axis. Data were acquired continuously over 12:50 min. Respiratory-resolved images were reconstructed off-line using compressed sensing and retrospective self-gating. Reconstructions were performed with a nominal resolution of 0.9 mm and a reduced isotropic resolution of 1.75 mm corresponding to shorter simulated scan times of 8:34 and 4:17 min, respectively. Analysis of apparent SNR was performed in all volunteers and reconstruction settings.

Results: The technique provided artifact-free morphologic lung images in all subjects. The short TR of bSTAR in conjunction with a field strength of 0.55 T resulted in a complete mitigation of off-resonance artifacts in the chest. Mean SNR values in healthy lung parenchyma for the 12:50 min scan were 3.6 ± 0.8 and 24.9 ± 6.2 for 0.9 mm and 1.75 mm reconstructions, respectively.

Conclusion: This study demonstrates the feasibility of morphologic lung MRI with a submillimeter isotropic spatial resolution in human subjects with bSTAR at 0.55 T.

KEYWORDS
0.55 T, balanced steady-state free precession, lung, non-Cartesian trajectories, radial MRI

1 | INTRODUCTION

High-resolution MRI of the lung remains challenging because of limited signal-to-noise despite the continuous advancements in hardware, acquisition techniques and image post-processing. Strong magnetic susceptibility differences at the mesoscopic scale of alveoli lead to a rapid T_2^* signal decay, particularly at clinical field strengths (>1.5 T).[1–3] This, in combination with the foam-like structure of the parenchyma, reflected by a low-proton density, leads to an overall poor SNR for lung MRI.[4,5] Additionally, respiratory and cardiac motion can further complicate data acquisition and negatively impact image quality and SNR. Recently, there has been a growing interest in exploring lung MRI on scanner configurations operating at lower field strengths with high performance gradient systems.[6–8] The lower field strength helps to reduce susceptibility artifacts and off-resonance artifacts, and therefore, provides more favorable transverse relaxation times.[9]

Despite the aforementioned technical difficulties of pulmonary MRI, significant efforts have been made in recent years to develop dedicated acquisition techniques for studying lung structure and function. In particular, imaging techniques based on UTE or zero echo time (ZTE) have shown promising results for lung imaging at 1.5 T and 3 T.[10–12] These techniques use non-Cartesian k-space trajectories, enabling improved sampling of the fast-decaying signal in tissues with very short T_2^*.

Another technique that has been demonstrated to be well-suited for lung imaging is balanced SSFP (bSSFP)[13]; a pulse sequence that has found its major application in cardiovascular imaging.[14] bSSFP is a rapid imaging technique in which the net gradient-induced dephasing over a TR interval is zero. It offers a unique T_2/T_1 contrast and highest SNR per unit time as compared to incoherent SSFP techniques.[15] Generally, however, bSSFP imaging can be demanding even on the modern clinical MR systems because it is prone to any source of imperfection that perturbs the perfectly balanced series of gradient pulses. Furthermore, bSSFP shows a pronounced sensitivity to off-resonance, leading to prominent signal drops in spatial regions with phase accruals close to $\phi = \pm 2\pi n \, (n \in N_0)$ known as "stop-bands" or "banding artifacts". These artifacts can be (partially) mitigated through proper shimming of the magnetic field (reducing the field inhomogeneity), or more simply, by shortening the TR. It was demonstrated that using state-of-the-art clinical MR systems, the TR could be close to the ~1 ms regime for 3D Cartesian bSSFP thoracic imaging at 1.5 T.[16] This technique provided diagnostic imaging quality with a moderate isotropic spatial resolution of approximately 2 mm in a single breath-hold.[17]

More recently, a non-Cartesian k-space sampling strategy based on a 3D half-radial bSSFP acquisition technique, termed bSTAR, has been proposed.[18] bSTAR uses dual-echo half-radial sampling by using bipolar gradients and non-selective radio frequency excitations, an acquisition scheme previously proposed by Diwoky et al.[19] The k-space is sampled with center-out and center-in half-radial projections following an Archimedean spiral trajectory in spherical coordinates. The pulse sequence offers an improved robustness against motion in comparison to the Cartesian readout. In addition, because slice encoding can be avoided it provides an increased sampling efficiency, SNR and spatial resolution with shortened TR. A recent study demonstrated compelling results for morphologic lung imaging in healthy volunteers at 1.5 T using a self-gated free-breathing 3D bSTAR.[20] The technique has been shown to provide artifact-free thorax images with an isotropic high spatial resolution of ~1.2 mm acquired in <5 min. The free-breathing bSTAR pulse sequence uses an interleaved wobbling Archimedean spiral pole (WASP) to ensure a homogenous k-space coverage with a uniform distribution of half-radial readouts over multiple breathing cycles. Furthermore, the WASP trajectory is designed to avoid large jumps in k-space, which can induce eddy currents and lead to severe image quality deterioration during bSSFP acquisitions.

Although the use of very short TR in bSSFP-based imaging techniques greatly reduces problems related to off-resonance, it also sets a limit on the maximum spatial resolution. Imaging at high spatial resolution requires lengthening of the readout, which increases TR, and generates unacceptable banding artifacts. However, this constraint can be significantly relaxed when imaging at 0.55 T. Additionally, dual-echo sampling of bSTAR can benefit from slowly decaying T_2^* species in the lung parenchyma at a lower magnetic field.[9] To this end, in this work we explore the potential of the free-breathing bSTAR technique for high-resolution morphologic lung MRI in human subjects using a 0.55 T MR-scanner equipped with high-performance gradients.

2 | METHODS

2.1 | Data acquisition

Five healthy volunteers (mean age: 28.4 years, range: 25–39 years, three males and two females) and a 74-year-old male patient with granulomatous lung disease were recruited to this study. Written informed consent was obtained from each subject before the examinations. The study was approved by the local Institutional Review Board. MRI experiments were performed

using a whole-body 0.55 T MR-system (prototype MAGNETOM Aera; Siemens Healthineers) equipped with high-performance shielded gradients (45 mT/m amplitude, 200 T/m/s slew rate). The integrated body coil was used for RF transmission and a combination of 6-channel body array (anterior) and 12-elements of the table-integrated spine array (posterior) was used for signal reception (Siemens Healthineers).

All subjects underwent morphological MRI with a 3D half-radial dual-echo bSTAR pulse sequence. The scans were performed in supine position during free breathing. The k-space data were sampled with an interleaved WASP trajectory.[20] The bSTAR scans were performed with a pre-defined shim setting at isocenter with the following parameters: FOV = 34 cm × 34 cm × 34 cm, twofold readout oversampling, TE1/TE2/TR = 0.13/1.93/2.14 ms, 200 μs hard RF pulse, flip angle = 20°, bandwidth = 1116 Hz/pixel, 0.90 mm nominal isotropic resolution based on k-space trajectory, 448 samples (896 with oversampling) per half-radial projection, 360 000 half-radial projections, 600 interleaves acquired in 12:50 min. For bSSFP the maximal signal is independent of TR,[21] so the TR was kept as short as possible while not exceeding gradient stimulation limits for the chosen spatial resolution. This maximizes the number of the radial projections acquired per time unit. For a smooth transition into steady state, a train of 500 dummy TRs with a constant flip angle was used before the data acquisition. No concomitant gradient correction was performed. Further technical details on the acquisition technique can be found in Bieri et al.[20]

To assess the image quality of bSTAR in absence of physiological noise with the proposed scanning protocol an accredited American College of Radiology (ACR) structural phantom was used.[22] The dimension of the phantom was 14.8 cm in length and 19 cm in diameter.

The deviations from the nominal k-space trajectory of the bSTAR scan were estimated by a calibration scan. The calibration was performed in a 14-cm diameter ball phantom by measuring the phase progression resulting from readout gradients oriented along each axis separately as proposed by Duyn et al.[23] Briefly, the gradient placed in the slice selection axis introduces spatially uniform time-varying changes in the resonant frequency on a slice at off-isocenter and the phase progression corresponds to the actual k-space trajectory. Instead of measuring all half-radial projections, the k-space trajectory correction of the radially acquired data was performed by measuring phase evolution during readout along each single axis along each single axis for positive and negative gradient polarities. As a result, six measurements were performed. The information from separate axes was combined to synthesize phase evolutions for all half-radial projections

as defined by an arbitrary azimuthal and polar angle in spherical coordinates.

For comparison, a thoracic CT scan of the patient with granulomatous lung disease performed 20 days before the MR examination was available. The low-dose thoracic CT was performed using a multidetector scanner (Aquilion 320, Toshiba). No contrast agent was administered. CT scanning parameters were as follows: helical acquisition, tube voltage = 120 kV, tube current = 20 mA, tube current-time product = 5.5 mAs, pitch factor = 0.813, iterative reconstruction (AIDR 3D) with slice thickness 0.5 mm, and 1 mm and sharp kernel FC51.

2.2 | Image reconstruction and analysis

Image reconstruction and post-processing of bSTAR datasets were carried out offline. The acquired calibration scan was used to estimate the actual k-space trajectory for all acquired bSTAR scans. For self-gating of the free-breathing scans, the respiratory signal modulation in the k-space center was automatically picked up from the chest and spine phased arrays using randomized singular value decomposition (rSVD).[20,24] The extracted respiratory signal modulation was then used to select 30% of the readouts acquired during the end-expiratory phase of the breathing cycle for image reconstruction. Subsequently, bSTAR datasets were reconstructed using compressed sensing with a fast iterative shrinkage thresholding algorithm (FISTA).[25] The data acquired at both echoes (i.e., obtained from the center-out and center-in half-radial projections) was reconstructed separately and combined by a voxelwise complex-valued addition. The in vivo scans were reconstructed at two spatial resolutions: 0.9 mm nominal isotropic resolution (matrix 512^3) and 1.75 mm isotropic resolution (matrix 320^3). Additionally, to explore the minimum required acquisition time, the in vivo datasets were reconstructed with 2/3 and 1/3 of the acquired readouts, which resulted in simulated reduced scan times of 8:34 min (240 000 readouts) and 4:17 min (120 000 readouts). The phantom dataset was reconstructed with 0.9 mm nominal isotropic resolution using the readouts selected for the end-expiratory reconstruction in volunteer 1. Furthermore, maximum intensity projection (MIP) images were calculated for visualization of the pulmonary vasculature. The reconstruction took ~6 min for 10 FISTA iterations, from which 2.5 min were spent on reading the datasets, generating the k-space trajectory, and performing self-gating. The in-house developed software for image reconstruction was written in C++ (GNU Compiler Collection 12.2 64-bit on Linux operating system), CUDA Toolkit 12.0 (NVIDIA),

and ITK library 5.2.[26] The reconstruction workstation was equipped with 2x Epyc 7502 CPU (AMD) and Quadro RTX 8000 GPU (NVIDIA).

Apparent SNR (aSNR) analysis was performed in all healthy volunteers for datasets with both spatial resolutions and with all three scan times. aSNR was calculated as the ratio of mean signal in the region of interest (ROI) by mean signal of noise-only region outside the volunteer's body. ROIs were placed on axially reformatted images by manually segmenting the pulmonary trunk and the lung parenchyma without vessels. The placement of the ROIs is shown in Figure S1. Calculations of aSNR were performed using ImageJ software (National Institutes of Health).

3 | RESULTS

The quality of image reconstruction in a phantom without the presence of physiological noise is shown in Figure 1. Representative thorax images from bSTAR datasets acquired in two healthy volunteers (1 and 2) and reconstructed with 0.9 mm nominal isotropic resolution in the end-expiratory phase of the respiratory cycle are presented in Figure 2. The figure includes coronal, sagittal, and axial views as well as MIP reconstructions with 15 mm thickness. High-spatial resolution allows for a detailed visualization of pulmonary structures. Additionally, a gravity-dependent signal gradient along the anterior–posterior direction in supine position can be observed on sagittal and axial views. Neither banding artifacts nor artifacts caused by cardiac motion can be noticed in the thorax. The off-resonance artifacts are limited to the peripheral FOV region with strong gradient non-linearity and lower magnetic field homogeneity. The coronally reformatted high-resolution bSTAR acquisition from volunteer 2 has been animated in the Video S1. The animation shows a 0.9 mm isotropic reconstruction, a sliding window reconstruction with averaged 4.5 mm slice thickness and an MIP reconstruction with 10 mm thickness.

Figure 3 shows coronal images from six reconstructions of the dataset acquired in volunteer 3 with spatial resolution of 0.9 mm and 1.75 mm as well as acquisition times of 12:50 min, 8:34 min, and 4:17 min. As expected, the reduction in scan time results in an apparent visual increase of the noise in the images. Furthermore, because of higher k-space undersampling of the shortened scans (undersampling factor $[R] = 12.45$ for 4:17 min scan and $R = 6.22$ for 8:34 min scan vs. $R = 4.15$ for 12:50 min scan) there is a noticeable blurring visible on the 0.9 mm reconstruction. For each MIP reconstruction, the figure shows a small zoomed in lung region in a white box. The impact of the reduced scan time manifested as increased noise and decreased sharpness of the vascular structure, which can be clearly observed and is pronounced especially in the 4:17 min acquisition. Apparent SNR values measured in all volunteers in the lung parenchyma and pulmonary trunk for as reconstruction setups are reported in Table 1. The ratios of the aSNR estimated for 1.75 mm and 0.9 mm reconstructions are close to the theoretical value of ∼7.3.

A comparison between the bSTAR and low-dose CT images obtained in patient with granulomatous lung disease is shown in Figure 4. Both datasets show corresponding slice locations in coronal, sagittal, and axial
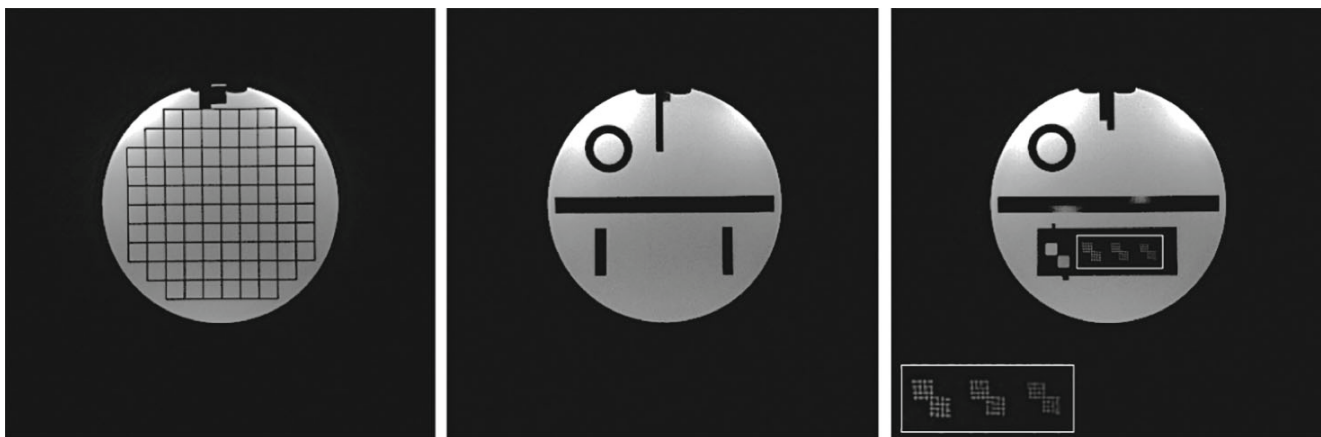

FIGURE 1 Illustrative balanced steady-state free precession with half-radial dual-echo readout (bSTAR) images of a structural phantom (American College of Radiology)[22] reconstructed with 0.9 mm isotropic resolution. To simulate realistic k-space sampling pattern half-radial readouts binned for the expiratory phase in volunteer 1 (30% of the acquired data) were used for the reconstruction. The resolution inserts (image on the right) has been marked with a white rectangle and zoomed in the left bottom corner for an improved visualization. The dimensions of the resolution inserts (from left to right): 0.9 mm, 0.8 mm and 0.7 mm.
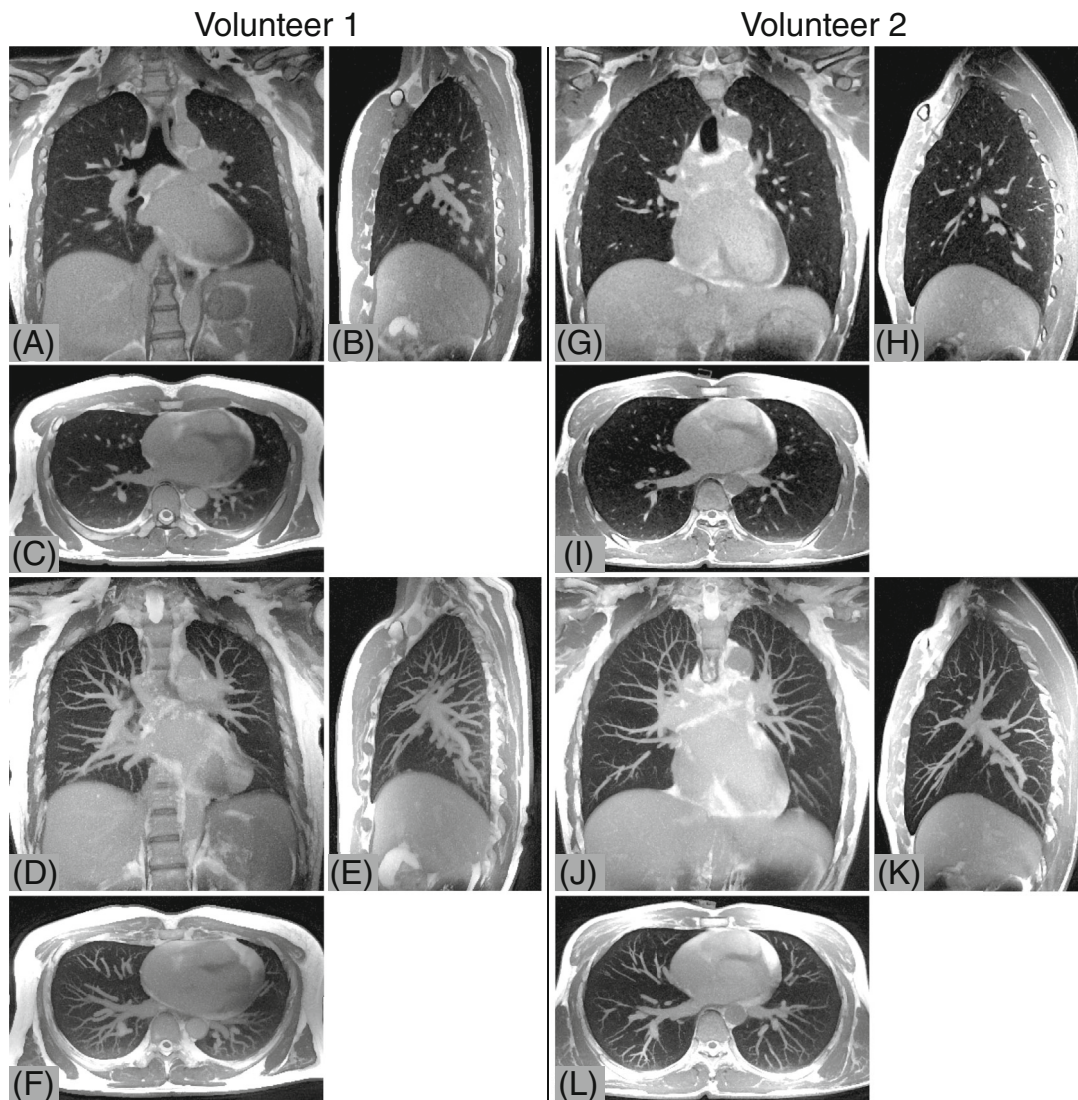
Volunteer 1   Volunteer 2

FIGURE 2 Illustrative thorax images obtained with free-breathing balanced steady-state free precession with half-radial dual-echo readout (bSTAR) in two volunteers (left: volunteer 1–39 year-old male, right: volunteer 2–34 year-old male) and reconstructed with 0.9 mm isotropic resolution. The upper part of the figure shows images in coronal (A,G), sagittal (B,H), and axial (C,I) views. The bottom part of the figure presents maximum intensity projection (MIP) images reconstructed with 15 mm thickness in in coronal (D,J), sagittal (E,K), and axial views (F,L).

views. Lung pathologies including partially calcified bilateral upper lobe pulmonary masses, bronchiectatic changes, bronchial wall thickening in the right upper lobe as well as pulmonary bullae, can be recognized on both scans.

4 | DISCUSSION

In this work, we investigated a free-breathing self-gated 3D bSSFP imaging technique, termed bSTAR, for the assessment of lung morphology in human subjects on a high-performance 0.55 T MR-system. The imaging technique uses a simple minimal-TR bSSFP kernel generating two half-echoes and offering high acquisition efficiency (~85% of TR). The bSTAR technique benefits from the intrinsically high SNR offered by bSSFP as well as from the fact that there is very little signal intensity loss in the second echo.[27] However, for short lived T_2^* species, this effect is more pronounced at higher field strength, that is, at 1.5 T where T_2^* in the lung parenchyma is in order of 1–2 ms, compared to 0.55 T where T_2^* in the lung tissue is ~8 ms.[9]

The feasibility of bSTAR was successfully presented at 1.5 T in healthy human subjects[20] and provided free-breathing chest images with 1.2 mm isotropic resolution in <5 min. There scans were performed with undersampling factor of 7.5, which is close to the
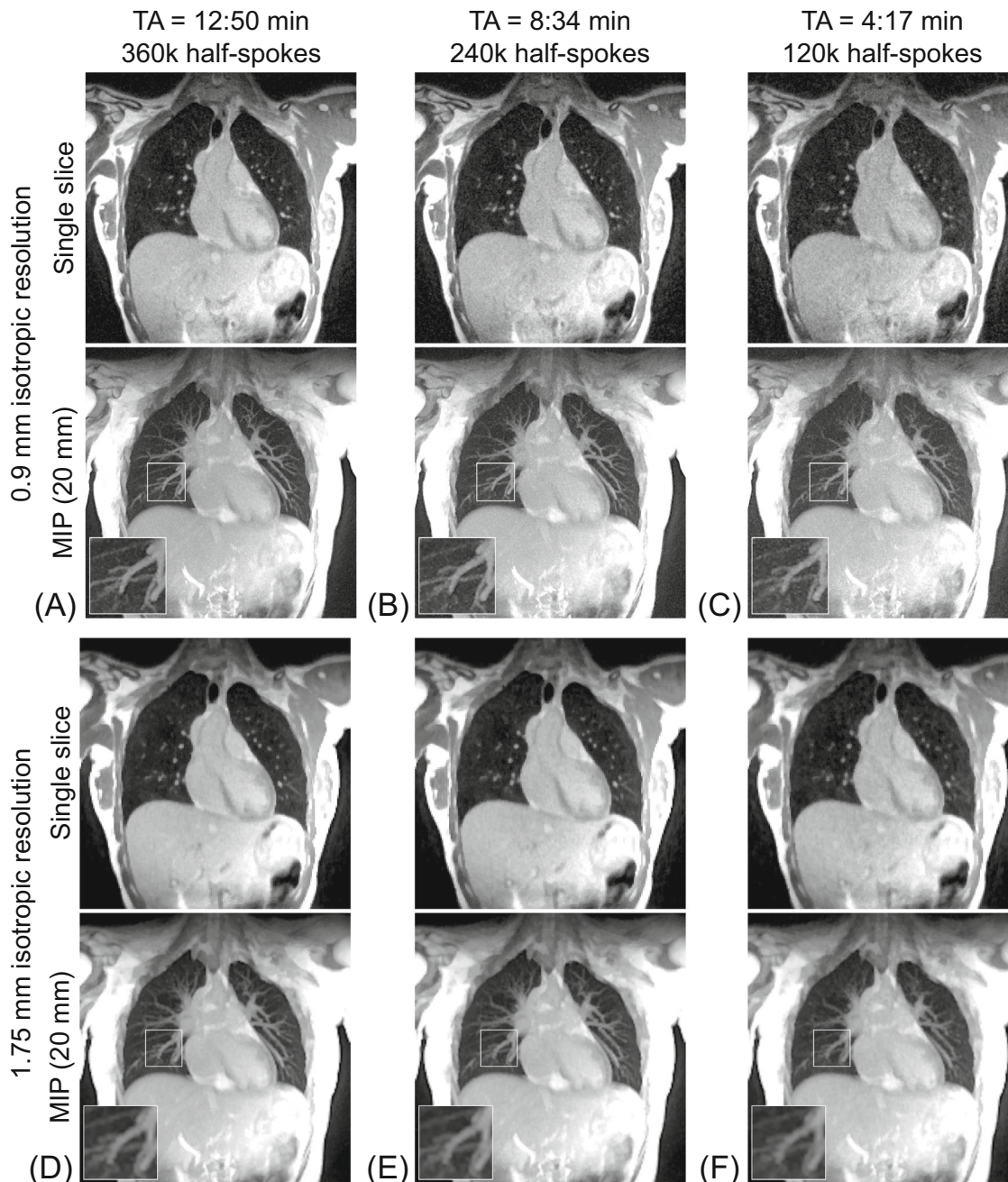
FIGURE 3 Comparison between image reconstructions from the data acquired in volunteer 3 (26 year-old female) with 0.9 mm (A–C) and 1.75 mm (D–F) isotropic resolution for single coronal slices and maximum intensity projection (MIP) images reconstructed with 20 mm thickness. The reconstructions were performed using all data with the scan time of 12:50 min (A,D), and simulated scan times of 8:34 min (B,E) and 4:17 min (C,F). The apparent SNR values measured in the lung parenchyma were as follows: 4.0 for 12:50 min, 3.4 for 8:34 min, and 2.7 for 4:17 min scan with 0.9 mm reconstruction, and 22.8 for 12:50 min, 20.7 for 8:34 min, and 15.7 for 4:17 min scan with 1.75 mm reconstruction.

undersampling factor of 8.3 used in this work for the 12:50 min bSTAR scan. The main constraint for the bSTAR technique at 1.5 T is the requirement for extremely short TR in a range of ∼1.0 to 1.5 ms and a good B_0 homogeneity to avoid off-resonance artifacts in a large FOV used for chest imaging. Additionally, short TRs necessitate the use of short readouts with high amplitude and bandwidth, which limits the maximal achievable spatial resolution. To this end, bSSFP-based techniques are especially well suited for imaging at lower magnetic field strength such as 0.55 T. The lower magnetic field provides not only more favorable transverse relaxation times for the lung tissue, but also loosens the requirement of very short TRs for mitigation of the off-resonance artifacts. Moreover, despite

TABLE 1 Apparent SNR values measured in lung parenchyma and pulmonary trunk in all volunteers in images with 0.9 mm and 1.75 mm isotropic resolution reconstructed using all acquired data and simulated shortened scan times.

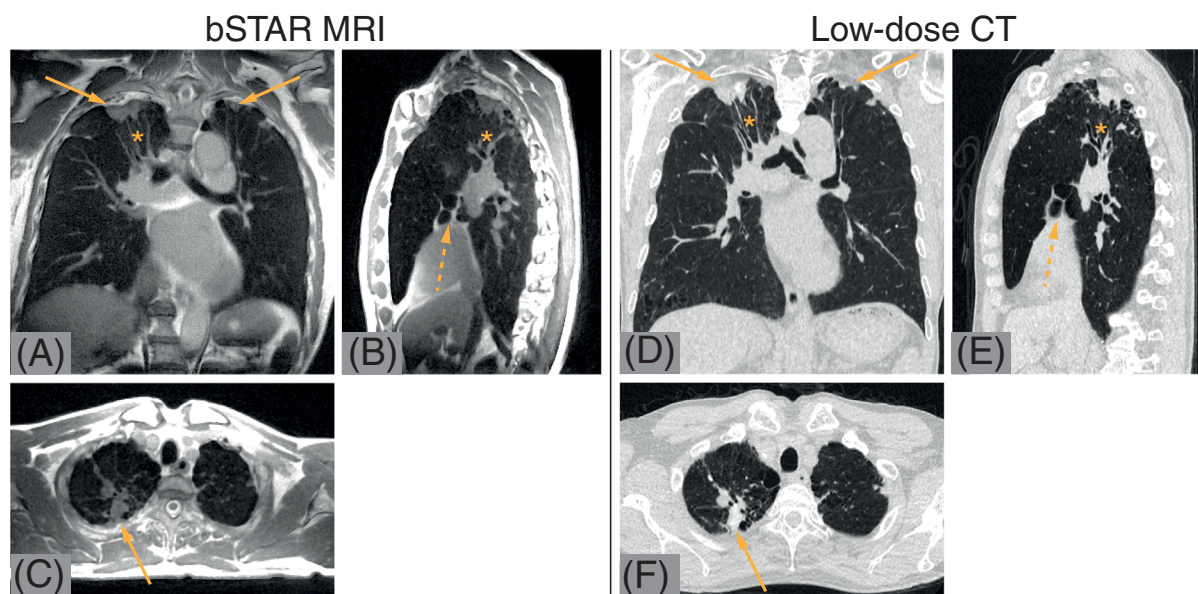| Region of interest	Spatial resolution					
	0.9 mm			1.75 mm		
	12:50 min	8:34 min	4:17 min	12:50 min	8:34 min	4:17 min
Lung parenchyma	3.6 ± 0.8	3.0 ± 0.8	2.4 ± 0.5	24.9 ± 6.2	21.9 ± 5.6	16.9 ± 3.8
Pulmonary trunk	13.1 ± 0.2	11.2 ± 0.3	9.3 ± 0.4	91.9 ± 5.3	79.7 ± 5.6	62.9 ± 3.3

bSTAR MRI   Low-dose CT

FIGURE 4 Coronal (A,D), sagittal (B,E), and axial (C,F) thorax images acquired with free-breathing balanced steady-state free precession with half-radial dual-echo readout (bSTAR) MRI (0.9 mm isotropic resolution, TA = 12:50 min) and low-dose CT in 74-year-old patient with granulomatous lung disease. Both scans show partially calcified bilateral upper lobe pulmonary masses (solid arrows), bronchiectatic changes and bronchial wall thickening in the right upper lobe (orange asterisks) as well as pulmonary bullae (dashed arrows).

the lower spin polarization at 0.55 T compared to clinical field strengths, the application of bSSFP with its inherently high signal amplitude compensates the signal loss associated with spoiling of the transverse magnetization in SPGR-based techniques.

Recently, it has been shown that free-breathing bSTAR imaging is feasible at 0.55 T using a low-cost and low-performance clinical MR-scanner.[28] The pilot study was conducted in sarcoidosis patients with a nominal isotropic resolution of 1.3 mm in a clinically acceptable scan time of only 6 min. In this study, we have shown that the combination of the beneficial factors associated with imaging at 0.55 T together with a high-performance gradient system enables a submillimeter (0.9 mm) isotropic spatial resolution with bSTAR for the assessment of lung morphology. The pulse sequence provided artifact-free images allowing for a detailed visualization of pulmonary structures or a lung pathology.

One of the main limitations of this technique is a relatively long acquisition time of over 12 min required for a submillimeter scan. By simulating other scan times from complete datasets, we showed that it is possible to shorten the acquisition time by about one-third with a slight loss in aSNR and sharpness in visualization of the pulmonary vessels. An important advantage of an isotropic non-Cartesian scan is the possibility of regridding the data onto an arbitrary matrix size. Consequently, the matrix size and spatial resolution can be reduced to a moderate resolution of 1.75 mm as presented in this manuscript if higher aSNR in the lung parenchyma is required 9e.g. for identification of regions with air-trapping or emphysematous changes.

Another limitation is associated with the self-gating method used in this work. In fact, only part of the data (∼30%) was used to reconstruct the expiratory phase of the respiratory cycle. Furthermore, we did not detect

bulk motion in the data, which can severely affect the reconstruction quality. Hence, our technique can benefit from more advanced post-processing such as iterative motion-compensation reconstruction[29] or recently presented self-supervised model based deep learning method.[30]

5 | CONCLUSION

In this study, we demonstrated the feasibility of sub-millimeter lung imaging using respiratory self-gated bSTAR MRI in human subjects on a 0.55 T MR-system. The bSTAR technique profits from maximal sampling efficiency as well as from a high intrinsic SNR offered by bSSFP. Data acquisition at 0.55 T helped to successfully mitigate off-resonance artifacts and allows for artifact-free imaging with a submillimeter isotropic spatial resolution. Future studies will focus on the exploration of the clinical added value of the free breathing bSTAR technique in patients with pulmonary disease.

ORCID
Grzegorz Bauman https://orcid.org/0000-0001-6972-0776
Nam G. Lee https://orcid.org/0000-0001-5462-1492
Ye Tian https://orcid.org/0000-0002-8559-4404
Oliver Bieri https://orcid.org/0000-0002-6755-5495
Krishna S. Nayak https://orcid.org/0000-0001-5735-3550

TWITTER
Grzegorz Bauman @radphysusb

REFERENCES
1. Hatabu H, Alsop DC, Listerud J, Bonnet M, Gefter WB. T2* and proton density measurement of normal human lung parenchyma using submillisecond echo time gradient echo magnetic resonance imaging. *Eur J Radiol.* 1999;29:245-252.
2. Hatabu H, Gaa J, Tadamura E, et al. MR imaging of pulmonary parenchyma with a half-Fourier single-shot turbo spin-echo (HASTE) sequence. *Eur J Radiol.* 1999;29:152-159.
3. Bauman G, Santini F, Pusterla O, Bieri O. Pulmonary relaxometry with inversion recovery ultra-fast steady-state free precession at 1.5T. *Magn Reson Med.* 2017;77:74-82.
4. Wild JM, Marshall H, Bock M, et al. MRI of the lung (1/3): methods. *Insights Imaging.* 2012;3:345-353. doi:10.1007/s13244-012-0176-x
5. Biederer J. MR imaging of the airways. *Br J Radiol.* 2023;96:20220630. doi:10.1259/bjr.20220630
6. Bhattacharya I, Ramasawmy R, Javed A, et al. Oxygen-enhanced functional lung imaging using a contemporary 0.55 T MRI system. *NMR Biomed.* 2021;34:e4562. doi:10.1002/nbm.4562
7. Seemann F, Javed A, Chae R, et al. Imaging gravity-induced lung water redistribution with automated inline processing at 0.55 T cardiovascular magnetic resonance. *J Cardiovasc Magn Reson.* 2022;24:35. doi:10.1186/s12968-022-00862-4
8. Javed A, Ramasawmy R, O'Brien K, et al. Self-gated 3D stack-of-spirals UTE pulmonary imaging at 0.55T. *Magn Reson Med.* 2022;87:1784-1798. doi:10.1002/mrm.29079. Erratum in: *Magn Reson Med* 2022 Nov;88:2326–2327.
9. Li B, Lee NG, Cui SX, Nayak KS. Lung parenchyma transverse relaxation rates at 0.55 T. *Magn Reson Med.* 2023;89:1522-1530. doi:10.1002/mrm.29541
10. Johnson KM, Fain SB, Schiebler ML, Nagle S. Optimized 3D ultrashort echo time pulmonary MRI. *Magn Reson Med.* 2013;70:1241-1250. doi:10.1002/mrm.24570
11. Wielputz MO, Triphan SMF, Ohno Y, Jobst BJ, Kauczor HU. Outracing lung signal decay – potential of ultrashort echo time MRI. *Rofo.* 2019;191:415-423.
12. Bae K, Jeon KN, Hwang MJ, et al. Comparison of lung imaging using three-dimensional ultrashort echo time and zero echo time sequences: preliminary study. *Eur Radiol.* 2019;29:2253-2262.
13. Bieri O, Scheffler K. Fundamentals of balanced steady state free precession MRI. *J Magn Reson Imaging.* 2013;38:2-11.
14. Ismail TF, Strugnell W, Coletti C, et al. Cardiac MR: from theory to practice. *Front Cardiovasc Med.* 2022;9:826283. doi:10.3389/fcvm.2022.826283
15. Scheffler K, Lehnhardt S. Principles and applications of balanced SSFP techniques. *Eur Radiol.* 2003;13:2409-2418.
16. Bieri O. Ultra-fast steady state free precession and its application to in vivo (1)H morphological and functional lung imaging at 1.5 Tesla. *Magn Reson Med.* 2013;70:657-663. doi:10.1002/mrm.24858
17. Heye T, Sommer G, Miedinger D, Bremerich J, Bieri O. Ultrafast 3D balanced steady-state free precession MRI of the lung: assessment of anatomic details in comparison to low-dose CT. *J Magn Reson Imaging.* 2015;42:602-609. doi:10.1002/jmri.24836
18. Bauman G, Bieri O. Balanced steady-state free precession thoracic imaging with half-radial dual-echo readout on smoothly interleaved archimedean spirals. *Magn Reson Med.* 2020;84:237-246. doi:10.1002/mrm.28119
19. Diwoky C, Liebmann D, Neumayer B, et al. Positive contrast of SPIO-labeled cells by off-resonant reconstruction of 3D radial half-echo bSSFP. *NMR Biomed.* 2015;28:79-88. doi:10.1002/nbm.3229
20. Bieri O, Pusterla O, Bauman G. Free-breathing half-radial dual-echo balanced steady-state free precession thoracic imaging with wobbling Archimedean spiral pole trajectories. *Z Med Phys.* 2022;18:S0939-3889(22)00003-4. doi:10.1016/j.zemedi.2022.01.003
21. Reeder SB, Herzka DA, McVeigh ER. Signal-to-noise ratio behavior of steady-state free precession. *Magn Reson Med.* 2004;52:123-130. doi:10.1002/mrm.20126
22. Ihalainen TM, Lönnroth NT, Peltonen JI, et al. MRI quality assurance using the ACR phantom in a multi-unit imaging center. *Acta Oncol.* 2011;50:966-972.

23. Duyn JH, Yang Y, Frank JA, van der Veen JW. Simple correction method for k-space trajectory deviations in MRI. *J Magn Reson.* 1998;132:150-153. doi:10.1006/jmre.1998.1396

24. Halko N, Martinsson PG, Tropp JA. Finding structure with randomness: probabilistic algorithms for constructing approximate matrix decompositions. *SIAM Rev.* 2009;53:217-288.

25. Beck A, Teboulle M. A fast iterative shrinkage-thresholding algorithm for linear inverse problems. *SIAM J Imaging Sci.* 2009;2:183-202.

26. McCormick M, Liu X, Jomier J, Marion C, Ibanez L. ITK: enabling reproducible research and open science. *Front Neuroinform.* 2014;8:13. doi:10.3389/fninf.2014.00013

27. Ganter C. Static susceptibility effects in balanced SSFP sequences. *Magn Reson Med.* 2006;56:687-691.

28. Breit HC, Bauman G. Morphologic and functional assessment of sarcoidosis using low-field MRI. *Radiology.* 2022;303:255. doi:10.1148/radiol.211760

29. Zhu X, Chan M, Lustig M, Johnson KM, Larson PEZ. Iterative motion-compensation reconstruction ultra-short TE (iMoCo UTE) for high-resolution free-breathing pulmonary MRI. *Magn Reson Med.* 2020;83:1208-1221. doi:10.1002/mrm.27998

30. Miller Z, Johnson KM. Motion compensated self supervised deep learning for highly accelerated 3D ultrashort Echo time pulmonary MRI. *Magn Reson Med.* 2023;89:2361-2375. doi:10.1002/mrm.29586

SUPPORTING INFORMATION

Additional supporting information may be found in the online version of the article at the publisher's website.

Figure S1. Regions of interest placed on axial bSTAR images used for the calculation of the apparent SNR: blue area - segmented lung parenchyma without large vessels, yellow rectangle - noise-only region outside the volunteer's body, red area - segmented pulmonary trunk.

Video S1. Animation showing coronal reconstructions of freebreathing bSTAR acquisition obtained in volunteer #2 (left - 0.9 mm isotropic reconstruction, center - reconstruction with averaged 5 mm slice thickness, right - 10 mm maximum intensity projection).

Video Caption.